Fishnet model for failure probability tail of nacre-like imbricated lamellar materials

Wen Luo[a] and Zdeněk P. Bažant[a,b,c,1]

[a]Department of Mechanical Engineering, Northwestern University, Evanston, IL 60208; [b]Department of Civil Engineering, Northwestern University, Evanston, IL 60208; and [c]Department of Materials Science, Northwestern University, Evanston, IL 60208

Contributed by Zdeněk P. Bažant, October 27, 2017 (sent for review August 10, 2017; reviewed by Ross Corotis, George Deodatis, and Arash Yavari)

Nacre, the iridescent material of the shells of pearl oysters and abalone, consists mostly of aragonite (a form of $CaCO_3$), a brittle constituent of relatively low strength ($\approx$10 MPa). Yet it has astonishing mean tensile strength ($\approx$150 MPa) and fracture energy ($\approx$350 to 1,240 J/m^2). The reasons have recently become well understood: (*i*) the nanoscale thickness ($\approx$300 nm) of nacre's building blocks, the aragonite lamellae (or platelets), and (*ii*) the imbricated, or staggered, arrangement of these lamellea, bound by biopolymer layers only $\approx$25 nm thick, occupying $<$5% of volume. These properties inspire manmade biomimetic materials. For engineering applications, however, the failure probability of $\leq 10^{-6}$ is generally required. To guarantee it, the type of probability density function (pdf) of strength, including its tail, must be determined. This objective, not pursued previously, is hardly achievable by experiments alone, since $>10^8$ tests of specimens would be needed. Here we outline a statistical model of strength that resembles a fishnet pulled diagonally, captures the tail of pdf of strength and, importantly, allows analytical safety assessments of nacreous materials. The analysis shows that, in terms of safety, the imbricated lamellar structure provides a major additional advantage—$\sim$10% strength increase at tail failure probability 10^{-6} and a 1 to 2 orders of magnitude tail probability decrease at fixed stress. Another advantage is that a high scatter of microstructure properties diminishes the strength difference between the mean and the probability tail, compared with the weakest link model. These advantages of nacre-like materials are here justified analytically and supported by millions of Monte Carlo simulations.

failure probability | biomimetic materials | fracture mechanics | strength | size effect

The imbricated arrangement of the lamellae in nacreous structures is seen in Fig. 1 and is schematically idealized, without microscale disorder, in Fig. 2. The deterministic strength and fracture properties of nacre have been clarified by Suo, Gao and others in refs. 1–7. The mechanical robustness of Strombus gigas shells (or conch), which is similar to nacre, has been studied by Ballarini and coworkers (4, 8). A truss arrangement similar to Fig. 2*B* was used in ref. 5 as a replacement of bond layers in deterministic failure analysis.

For the purpose of statistical analysis, the longitudinal load transmission must be realistically simplified. Almost no load gets transmitted between the ends of adjacent lamellae in one row, and virtually all of the load gets transmitted by shear resistance of ultra-thin biopolymer layers between parallel lamellae. The links of the lamellae in adjacent rows may be imagined as the lines connecting the lamellae centroids, as marked in Fig. 2*A*.

1. Load Transmission and Redistribution

The essence of load transmission may thus be characterized by a system of diagonal tensile links (Fig. 1*B*), which looks like a fishnet loaded in the diagonal direction and can be simulated by a finite element program for pin-jointed trusses. The transverse stiffness is found to be statistically unimportant and is neglected. Thus, the fishnet model is initially a mechanism in which all of the links collapse under longitudinal load into a single line (Fig. 2*C*) while retaining, crucially, the imbricated (or staggered) connections.

When a link in the fishnet fails, its stress gets redistributed into the adjacent links. To keep an analytical probabilistic model simple, the redistribution is handled deterministically. The equilibrium equations of fishnet nodes are finite difference equations. They may be approximated by a continuous differential equation, which turns out to be the Laplace equation (9), $\nabla^2_{(x,y)} u = 0$, where u is the longitudinal displacement of the fishnet nodes after continuum smoothing and (x, y) are longitudinal and transverse coordinates in the initial stress-free state (i.e., before the fishnet collapses into a line); x = longitudinal coordinate (in the load direction).

This governing equation is a special case of Navier's equations of linear elasticity with Poisson's ratio equal to 0. Solving this equation in polar coordinates (R, θ) for an infinite domain with a circular hole, one finds that the stresses decay as R_0/R, where R_0 is a characteristic length proportional to hole radius. This deterministic approximation is then used in an analytical solution of failure probability. In numerical simulations, though, the stress redistribution among the links is computed exactly.

2. Failure Probability of Fishnet Model

We consider the case of load control, for which the failure load is the maximum load, σ_{max}. We analyze rectangular fishnets with k rows and n columns, containing $N = k \times n$ links (Fig. 2*C*), loaded uniformly by uniaxial stress σ imposed at the ends of rows.

Significance

The astonishing strength enhancement in the nacre of pearl oyster, compared with its main constituent, the aragonite, has recently been explained by the nanostructure of overlapping nanoscale platelets—but only deterministically. It is also necessary to know the stress value for which the failure probability does not exceed 1 in a million. It is shown that, at such a low-failure probability, the nacre-like structures exhibit additional advantages. The strength increases by about 10%, while at fixed, correspondingly low, stress, the failure probability decreases by 1 to 2 orders of magnitude, compared with the standard (Weibullian) extrapolation from the deterministic prediction and coefficient of variation. These are advantages important for biomimetic engineering applications.

Author contributions: W.L. and Z.P.B. designed research; W.L. and Z.P.B. performed research; W.L. and Z.P.B. contributed new analytic tools; W.L. and Z.P.B. analyzed data; and Z.P.B. wrote the paper.

Reviewers: R.C., University of Colorado, Boulder; G.D., Columbia University; and A.Y., School of Civil and Environmental Engineering and The George W. Woodruff School of Mechanical Engineering, Georgia Institute of Technology.

The authors declare no conflict of interest.

[1]To whom correspondence should be addressed. Email: z-bazant@northwestern.edu.

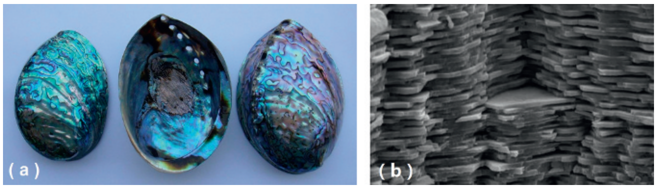

Fig. 1. (*A*) Nacre inside an abalone shell. (Image courtesy of Wikimedia Commons/Doka54.) (*B*) Electron microscopy image of a fractured surface of nacre. (Image courtesy of Wikimedia Commons/Fabian Heinemann.)

Let $P_f(\sigma)$ be the failure probability of fishnet loaded by σ and $X(\sigma)$ the total number of links failed at the end of the experiment under constant load σ. This means that $X(\sigma)$ is measured when no more damages occur. The failed links may be contiguous or scattered discontinuously. The events $\{X(\sigma) = r\}, r = 1, 2, 3, \dots$ are mutually exclusive (or disjoint). So to obtain the survival probability of the whole fishnet, the corresponding survival probabilities, $P_{S_r}(\sigma)$, must be summed:

$$1 - P_f(\sigma) = P_{S_0}(\sigma) + P_{S_1}(\sigma) + P_{S_2}(\sigma) + \cdots + P_{S_{k-1}}(\sigma) + \mathrm{Prob}(\mathrm{X}(\sigma) \geq \mathrm{k} \text{ and no through crack exists}) \quad \textbf{[1]}$$

where $P_f(\sigma) = \mathrm{Prob}(\sigma_{\max} \leq \sigma)$; σ_{max} is the nominal strength of structure; and $P_{S_r}(\sigma) = \mathrm{Prob}(\mathrm{X}(\sigma) = r),\ r = 0, 1, 2, \dots$.

The event $\{X(\sigma) = 0\}$ means that all N links survive (i.e., none fails) under load σ. With the notation $P_1(\sigma) = \mathrm{Prob}(\sigma_i \leq \sigma)$ = given failure probability of one link, the joint probability theorem yields $1 - P_{S_0}(\sigma) = [1 - P_1(\sigma)]^N$. This is equivalent to the weakest link chain model. Based on Eq. **1**, this model represents an upper bound on P_f of the fishnet. The link strengths are considered to be identical identically distributed (i.i.d.) random variables, which means that the autocorrelation length of the discrete field of link strengths is assumed not to be longer than the length of one link. This approximation is plausible because interlaminar bonds are separated by stiff lamellae and thus must have formed without any mutual influences.

As previously derived from bond break frequency, or probability, on the atomic scale, and from the laws of the nano–macro transition of power law probability tails under parallel and series couplings (10–14), the probability distribution on the level of one fishnet link must be the Gaussian distribution with a Weibull distribution grafted on the left, which, in the remote tail, is a power law of exponent m equal to Weibull modulus, m (typically, m lies between 20 and 50). For $N \to \infty$, $P_{S_0}(\sigma) = 1 - e^{-(\sigma/\sigma_0)^m}$ = the Weibull distribution (14, 15), which gives a straight line of slope m in the Weibull scale.

3. Two-Term Fishnet Statistics

To get a better upper bound, we now include the second term in Eq. **1**—that is, $1 - P_f(\sigma) = P_{S_0}(\sigma) + P_{S_1}(\sigma)$, where σ equals average longitudinal stress in the cross-section, the same in every section. The second term contributing to survival probability represents the joint probability that one and only one among N links fails while simultaneously all of the other links survive under load σ at the end of experiment. So, according to the joint probability theorem:

$$P_{S_1}(\sigma) = NP_1(\sigma) \cdot \prod_{i=1}^{N-1} [1 - P_1(\lambda_i \sigma)] \quad \textbf{[2]}$$

Here λ_i is the stress redistribution factor, which is, for simplicity, obtained deterministically; λ_i can be ≥ 1 or < 1. For the rest of $N - 1$ links to survive, they must first survive under the initial uniform stress field $\sigma_i = \sigma$ and then under the redistributed stress field $\sigma_i = \lambda_i \sigma$. Where $\lambda_i < 1$ (shielding zone), the links need to survive only the initial stress field, which means we can reset λ_i as 1.

For the sake of simplicity, we further assume that (*i*) the stress redistribution affects only a finite number, ν_1, of links in a finite neighborhood of the first failed link in which $\lambda_i > 1.1$ and (*ii*) factor λ_i is treated as constant, $\lambda_i = \eta_a^{(1)}$ (> 1) within this neighborhood, taken either as the weighted average of all redistribution factors (to get the best estimate) or as the maximum of these factors (to preserve an upper bound on P_f). With this simplification, Eq. **2** becomes:

$$P_{S_1}(\sigma) = NP_1(\sigma)[1 - P_1(\sigma)]^{N-\nu_1-1}[1 - P_1(\eta_a^{(1)}\sigma)]^{\nu_1} \quad \textbf{[3]}$$

Here N means that failure can start in any one of the N links, which gives N mutually exclusive cases. The two bracketed terms mean that the failure of one of the N links must occur jointly with the survival of (*i*) each of the remaining $(N - \nu_1 - 1)$ links with stress σ and (*ii*) each of the remaining ν_1 links with redistributed stress $\eta_a^{(1)}$.

In view of Eqs. **1** and **3**, the two-term estimate of P_f may be conveniently rearranged as:

$$1 - P_f(\sigma) = [1 - P_1(\sigma)]^N \quad \textbf{[4]}$$

$$\cdot \left\{1 + NP_1(\sigma)P_\Delta(\sigma, \eta_a^{(1)}, \nu_1)\right\} \quad \textbf{[5]}$$

where

$$P_\Delta = \frac{1}{1 - P_1(\sigma)}\left[\frac{1 - P_1(\eta_a^{(1)}\sigma)}{1 - P_1(\sigma)}\right]^{\nu_1} \quad \textbf{[6]}$$

Note that $P_\Delta \to 1$ as $\sigma \to 0$. Therefore, at the lower tail of P_f, we have:

$$1 - P_f(\sigma) = [1 - P_1(\sigma)]^N \cdot \{1 + NP_1(\sigma)\} \quad \textbf{[7]}$$

To help in understanding, Eq. **7** may be transformed to the Weibull plot of $Y^* = \ln[-\ln(1 - P_f)]$ versus $X^* = \ln\sigma$. Using, for small P_1, the second-order Taylor series approximation $\ln[1 - P_f(\sigma)] \simeq -N(N+1)P_1^2/2$, one obtains, for Weibull scale plot:

$$Y^* = 2\ln P_1(\sigma) + C, \quad C = \ln[N(N+1)] - \ln 2 \quad \textbf{[8]}$$

To compare, the Weibull scale plot for the weakest link model is $Y^* = \ln P_1(\sigma)$ + constant. So we conclude that the second

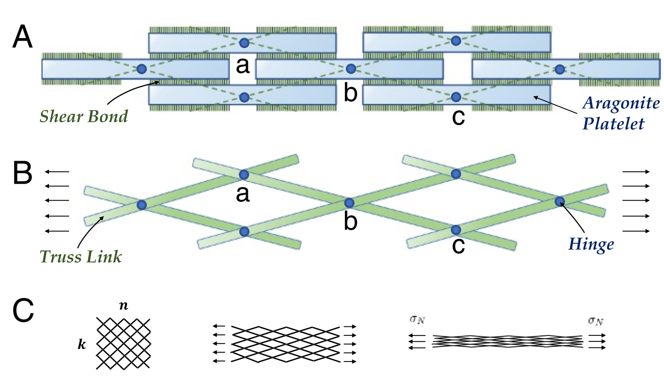

Fig. 2. (*A*) Schematic microstructure of nacre. (*B*) Equivalent fishnet structure with similar topology. (*C*) Deformation mechanism of transversely unconstrained fishnet.

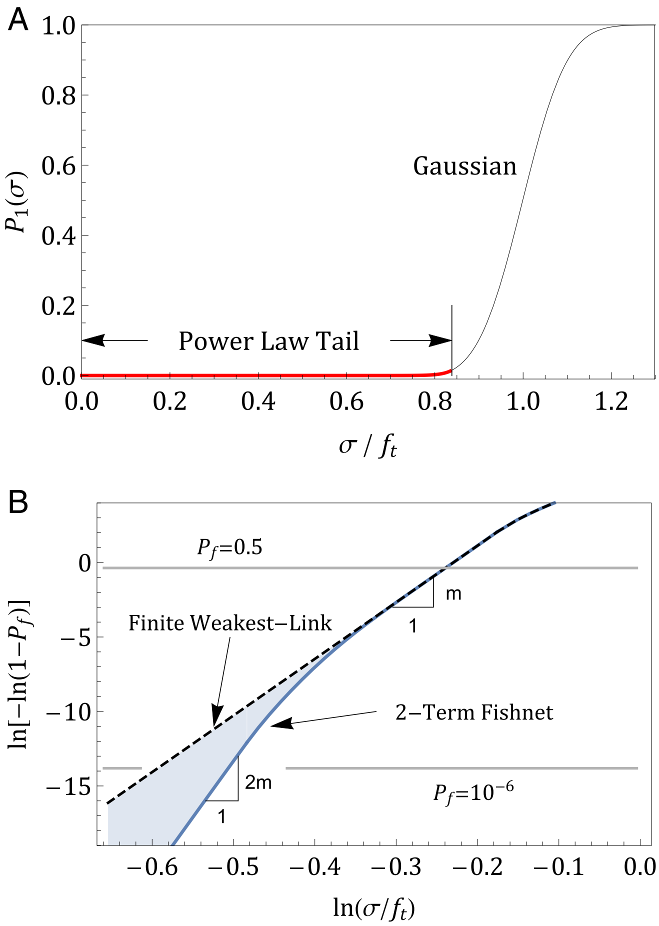

Fig. 3. (*A*) Cumulative distribution function (cdf) of failure for a single link with mean $f_t = 10.016$ MPa and coefficient of variation (CoV) = 7.8%. (*B*) Comparison of P_f (in Weibull scale) between the finite weakest link model and the fishnet model with the first two terms in the expansion of Eq. **1**.

term of fishnet statistics increases the terminal slope of strength probability distribution in the Weibull scale by a factor of 2.

Particularly important are the implications for structural safety. In Fig. 3*B*, the horizontal line for $P_f = 10^{-6}$ marks the maximum failure probability that is tolerable for engineering design. In this typical case, for constant N, the strength for $P_f = 10^{-6}$ is seen to increase by 10.5% when passing from the weakest link failures to fishnet failures, while, at fixed strength, the P_f is seen to decrease about 25 times. The P_f decrease depends on the fishnet configurations and P_1 but is generally more than 10-fold. This is an enormous safety advantage of the imbricated lamellar microstructure, which comes in addition to the advantages previously identified by deterministic studies.

Note that, for $\sigma \to \infty$, the term P_Δ in Eq. **6** approaches 0. This causes the strength probability for high σ to be close to the weakest link model, which corresponds to the first term of the sum in Eq. **1** (see Fig. 3).

The transition from slope m to $2m$ is approximately centered at stress σ_T for which $P_\Delta(\sigma_T) = 0.5$. Calculations show that the center of the transition shifts left and down dramatically as the redistribution factor $\eta^{(1)}$ is increased from 1.1 to 1.6.

4. Three-Term Fishnet Statistics

Further improvement can be obtained by including the third term of the sum in Eq. **1**. This term may be split into two parts, $P_{S_2} = P_{S_{21}} + P_{S_{22}}$, which are mutually exclusive and thus additive. They represent the survival probabilities when the next failed link is, or is not, adjacent to the previously failed link:

$$P_{S_{21}} = \binom{N}{1}\binom{\nu_1}{1}\int_{x_1=0}^{\sigma}\int_{x_2=x_1}^{\eta^{(1)}\sigma}\psi(x_1)\psi(x_2)\mathrm{d}x_2\mathrm{d}x_1 \quad \textbf{[9]}$$

$$\cdot[1-P_1(\sigma)]^{N-\nu_2-2}\left[1-P_1(\eta^{(2)}\sigma)\right]^{\nu_2} \quad \textbf{[10]}$$

$$P_{S_{22}} = \binom{N}{1}\binom{N-\nu_1-1}{1}\int_{x_1=0}^{\sigma}\int_{x_2=x_1}^{\sigma}\psi(x_1)\psi(x_2)\mathrm{d}x_2\mathrm{d}x_1 \quad \textbf{[11]}$$

$$\cdot[1-P_1(\sigma)]^{N-2\nu_1-2}\left[1-P_1(\eta^{(2)}\sigma)\right]^{2\nu_1} \quad \textbf{[12]}$$

Here $\psi(\sigma) = \mathrm{d}P_1(\sigma)/\mathrm{d}\sigma$ = pdf of the strength of each link; $\eta^{(2)}$ = stress redistribution ratio for links, ν_2 in number, adjacent to two failed links. This ratio is, for simplicity, assumed to be uniform over a zone where the redistributed stress exceeds 1.1σ.

When, in Eqs. **9–11**, the integral over x_2 is substituted into integrals from $x_2 = x_1$ to $x_2 = \sigma$ and from $x_2 = \sigma$ to $x_2 = \eta^{(1)}\sigma$, one gets:

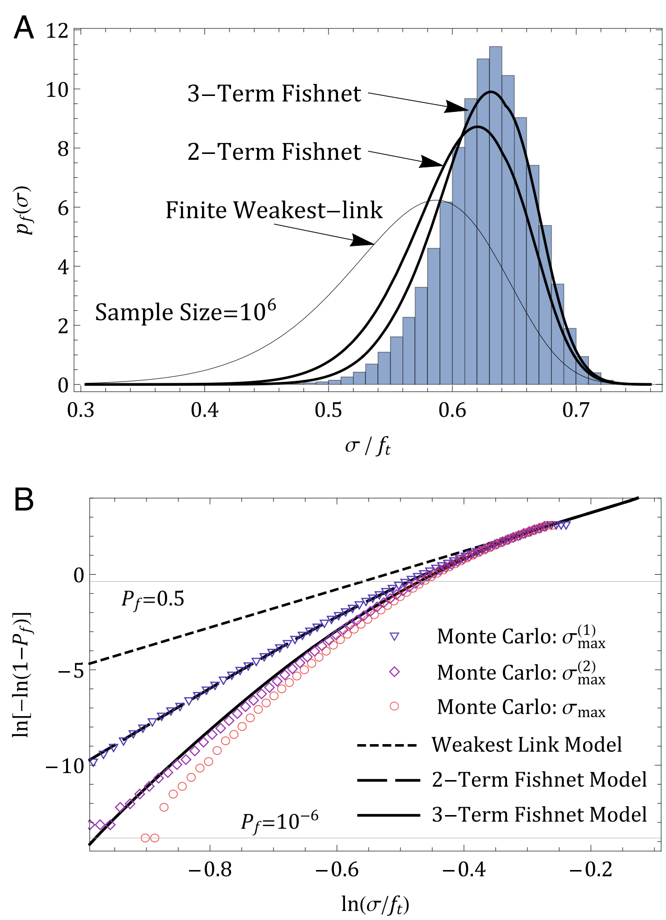

Fig. 4. (*A*) Normalized histogram of 10^6 Monte Carlo realizations (σ_{max}) compared with the probability density functions of the weakest link, two-term fishnet and three-term fishnet models. (*B*) The same data as well as the histogram of $\sigma^{(1)}_{max}$ and $\sigma^{(2)}_{max}$ converted into cumulative probability distribution and plotted on Weibull paper. f_t = 9.87 MPa is the mean strength of one link and CoV = 9.87%.

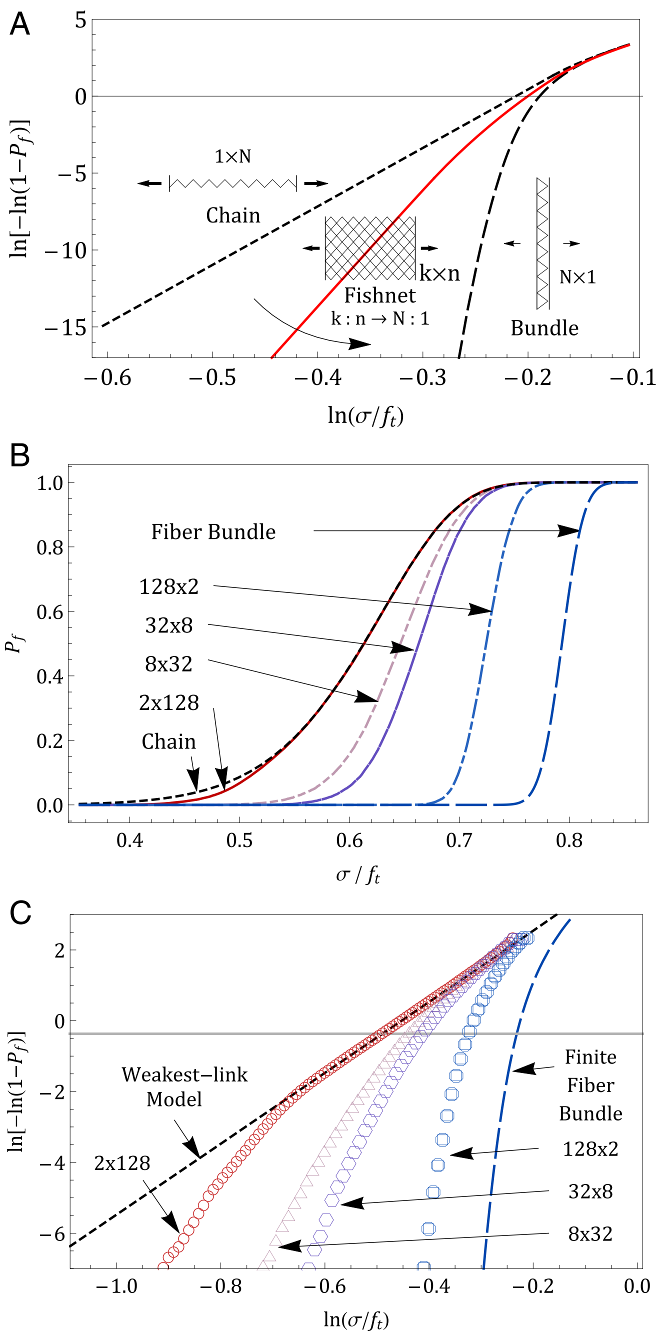

Fig. 5. (*A*) Change of failure probability of a fishnet pulled horizontally caused by varying the aspect ratio k/n gradually from 1 : N to N : 1 at constant number of links (Weibull scale). (*B*) Monte Carlo simulations showing the transition of P_f as the aspect ratio of fishnet is changed from $1 \times N$ to $N \times 1$ ($N = 256$). (*C*) The same data replotted on Weibull paper. $f_t = 9.87$ MPa is the mean strength of one link and CoV = 9.87%.

$$P_{S_{21}} = N\nu_1 \left\{ P_1(\sigma) P_1(\eta_b^{(1)}\sigma) - \frac{1}{2} {P_1}^2(\sigma) \right\} \quad \textbf{[13]}$$

$$\cdot [1 - P_1(\sigma)]^{N-\nu_2-2} \cdot [1 - P_1(\eta^{(2)}\sigma)]^{\nu_2} \quad \textbf{[14]}$$

$$P_{S_{22}} = \frac{1}{2} N(N - \nu_1 - 1) {P_1}^2(\sigma) \quad \textbf{[15]}$$

$$\cdot [1 - P_1(\sigma)]^{N-2\nu_1-2} \cdot [1 - P_1(\eta^{(2)}\sigma)]^{2\nu_1} \quad \textbf{[16]}$$

Here the multipliers N and $(N - \nu_1 - 1)$, representing the values of combinatorial coefficients $\binom{N}{1}$, $\binom{\nu_1}{1}$, and $\binom{N-\nu_1-1}{1}$, mean that, for the first and second link failures, there are N, and ν_1 or $N - \nu_1 - 1$, mutually exclusive possibilities. The integrals over the pdf of random strength of one link express the joint probability of two links failing. The second integral reflects the fact that the second link that fails cannot have a lower strength than the first one (which translates into the restriction $x_2 \geq x_1$, imposed by the lower limit of the second integral in Eq. **11**). The bracketed terms give the condition of simultaneous survival of the remaining links, both of which take into account the equivalent redistributed stresses. The term $\frac{1}{2}{P_1}^2(\sigma)$ ensues from integrating over a triangular domain in plane (x_1, x_2) bordered by line $x_2 = x_1$.

Factoring out $[1 - P_1(\sigma)]^N$ from the sum of Eqs. **13** and **15**, one can further show that, in the Weibull scale plot, the three-term fishnet model causes a tripling of the slope of lower-left asymptote of the strength pdf compared with the weakest link model. Furthermore, since $P_{S_{22}}$ is asymptotically proportional to N^2 and $P_{S_{21}}$ to N, it may also be concluded that, for large fishnets, $P_{S_{21}}$ is negligible and that the second link failure before σ_{max} mostly occurs far away from the first.

The case of survival when more than three links fail before σ_{max} is too unwieldy to benefit from analytical treatment. Nevertheless, it can be shown that the terms of the sum in Eq. **1** are, asymptotically, power laws with increasing integer exponents and rapidly decreasing magnitudes, similar to Taylor series.

5. Monte Carlo Failure Simulations

A rectangular fishnet truss, with k rows and n columns of identical links, has been simulated by a finite element program (in MatLab). For computational stability, the fishnet is loaded under displacement control, by incrementing equal longitudinal displacements u_0 at the right boundary. At the left boundary, the horizontal displacement is zero. The boundary nodes slide freely in the transverse direction. According to the arguments in refs. 10, 11, 13, 14, based on nanomechanics and scale transitions, the cdf of strength of each link, $P_1(\sigma)$, is assumed to be a Gaussian (or normal) distribution with a Weibull tail of exponent m grafted on the left at failure probability P_g (for $\sigma \to 0$, the cdf $\propto \sigma^m$). The strength of each of the $N = k \times n$ links is generated randomly according to $P_1(\sigma)$.

Fishnets of various sizes $N = k \times n$, with various numbers k of rows and n of columns, have been numerically simulated, and the maximum of the cross-sectional average (or nominal) stress σ at the boundary has been evaluated. When the loading increment exhausts the strength of any link, the link is deleted, which represents a brittle type of link failure (i.e., no gradual softening).

The strengths of links represent a discrete random field. As argued before, the autocorrelation length is assumed to be equal

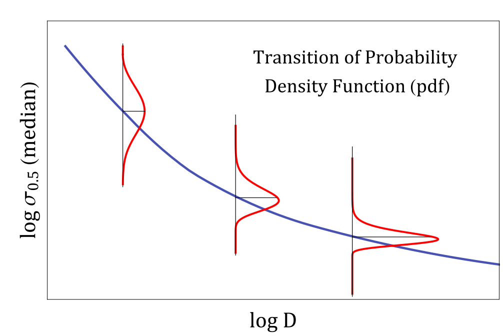

Fig. 6. Statistical size effect on the median strength of quasibrittle fishnet.

to the nodal spacing and may thus be ignored. Generally, about one million Monte Carlo simulations, for one million different random field inputs, have been run for each case and the maximum loads (or σ_{max})) have been recorded. Plotting, as a function of applied σ, the fraction of computed σ_{max} values that are less than various σ values, one gets the estimated cdf of fishnet strength. For one million random simulations, the normalized histogram gives an almost exact curve of the cdf of fishnet strength.

To verify the analytical two- or three-term statistics, respectively, the cases in which more than one, or two, links failed before the maximum load have been deleted from the set of about one million simulations of a fishnet having 16×32 links, CoV = 0.987 of P_1 and grafting point at $P_g = 0.09$. This is equivalent to omitting in Eq. **1** all of the terms except the first two or three, respectively. The remaining histograms ($\sigma_{max}^{(1)}$ and $\sigma_{max}^{(2)}$) are compared with the analytical cdf in Fig. 4*B* (Fig. 4*A* shows, for all simulations of σ_{max}, only the histogram). Despite simplifications, such as using a uniform redistribution ratio η and not distinguishing link failures at the boundary from those in the interior, the agreement is excellent. This validates the analytical solution.

For comparison, Fig. 4 also shows the histograms of all of the Monte Carlo simulations, which correspond to the complete sum in Eq. **1**. Note that, in this case, the three-term model, and even the two-term model, give a satisfactory estimate of fishnet cdf.

Consider now the effect of the fishnet shape or aspect ratio k/n. Fig. 5 shows the histograms obtained by random simulations (again about a million each) for fishnets with $N = 256$ links when their dimensions $k \times n$ are varied from 2×128, which represents the weakest link chain (or series coupling), to 128×2, which represents the fiber bundle (or parallel coupling, with mechanics-based load sharing—that is, equal extensions of all fibers). Obviously, the shape effect is enormous. However, fishnets with $k \gg n$ and rigid-body boundary displacements are not relevant to practical situations.

The simulations reveal that, for small enough CoV of strength, and particularly for a thin enough lower tail of $P_1(\sigma)$) (i.e., small enough P_g), the fishnet follows the weakest link model—that is, reaches the maximum load (and fails if the load is controlled) as soon as one link fails. The higher the CoV of link strength, the higher the number of links that tend to fail before reaching σ_{max}. This trend causes the left asymptote of cdf in Weibull plot to become steeper, as already shown in Fig. 4. Therefore, producing a high scatter (i.e., a higher CoV of $P_1(\sigma)$) of lamellar strength in biomimetic nacre-like structures will increase, relative to the weakest link model, the load corresponding to $P_f = 10^{-6}$, which governs safety (the abalone and pearl shells, as well as conch, already discovered that). An increased scatter, though, may decrease the mean strength, because of higher redistributed stress values induced by more numerous previous scattered damages.

Upon increasing the microstructural scatter, characterized by the CoV of the pdf of strength (which means increasing the thickness of the lower tail of P_1, by increasing the P_g), computations show that the fishnet tends to fail after the failure of an increasing number of links. So the failure zone size increases with microstuctural scatter. This means that the size of the fracture process zone (FPZ) and thus also the size of the representative volume element (RVE) are not constant, unless we consider only fishnets of the same degree of microstuctural scatter. In this respect, nacre differs from concrete, tough ceramics, fiber composites, rocks, sea ice, and many other quasibrittle materials, for which the size of RVE or a fully developed FPZ is approximately constant (14, 16).

6. Size Effect

For simplicity, the effect of fishnet size D (chosen either as k or n) at constant shape k/n is here studied only for the median strength, $\sigma_{0.5}$, rather than the mean strength, $\bar{\sigma}$. Both analytical considerations and computer simulations show that the size effect curve in the plot of $\log \sigma_{0.5}$ versus $\log D$ is not a straight line, as in Weibull theory. Rather, the curve descends at a decreasing slope. Also, the CoV of $\sigma_{0.5}$ decreases with size D (see Fig. 6). This is all similar to the type 1 size effect in fracture of concrete, rock, tough ceramics, fiber composites, and other quasibrittle materials.

More detailed results for the size effect and other aspects are beyond the scope of this study and will be presented in a separate more detailed paper (9). Further refinements and extensions, such as 3D generalization and quantification of $P_1(\sigma)$, will also be needed (14).

Conclusions

i) In addition to the weakest link chain and the fiber bundle, the fishnet is the third probabilistic strength model that is tractable analytically. It includes both former models as the limit cases.

ii) The analytical results on failure probability of fishnet are verified by Monte Carlo simulations of fishnets of various types, with about a million random simulations for each.

iii) The larger the scatter of link strength, the higher the number of links that are likely to fail before reaching the maximum load.

iv) The foregoing property brings about an important statistical advantage of fishnet connectivity in the microstucture—for increasing scatter in link strength (and probably also in the overlap length of adjacent lamellae), the cumulative probability distribution exhibits, in Weibull plot, an increasingly steeper lower left tail compared with the weakest link model. This greatly decreases the ratio of mean failure stress to the stress with failure probability 10^{-6}, which is beneficial for structural safety.

v) For the same number of links, the curve of cumulative probability distribution of fishnet lies, in Weibull plot, between the curves for the weakest link chain and the fiber bundle.

vi) As the longitudinal-to-transverse ratio of the number of links in a rectangular fishnet decreases, the probability distribution transits from the weakest link chain to the fiber bundle as the ratio increases.

vii) The fishnet strength exhibits a significant size effect when scaled up geometrically. The size effect is similar though not identical to the type 1 size effect (14) in concrete, tough ceramics, rocks, sea ice, fiber composites, and other quasibrittle materials.

ACKNOWLEDGMENTS. Partial financial support under Army Research Office Grant W911NF-15-1-0240 and NSF Grant N00014-11-1-0515, both to Northwestern University, is gratefully appreciated.

1. Wang R, Suo Z, Evans A, Yao N, Aksay I (2001) Deformation mechanisms in nacre. *J Mater Res* 16:2485–2493.
2. Gao H, Ji B, Jäger IL, Arzt E, Fratzl P (2003) Materials become insensitive to flaws at nanoscale: Lessons from nature. *Proc Natl Acad Sci USA* 100:5597–5600.
3. Shao Y, Zhao HP, Feng XQ, Gao H (2012) Discontinuous crack-bridging model for fracture toughness analysis of nacre. *J Mech Phys Solids* 60:1400–1419.
4. Ballarini R, Heuer AH (2007) Secrets in the shell the body armor of the queen conch is much tougher than comparable synthetic materials. What secrets does it hold? *Am Sci* 95:422–429.
5. Askarinejad S, Rahbar N (2015) Toughening mechanisms in bioinspired multilayered materials. *J R Soc Interface* 12:20140855.
6. Dutta A, Tekalur SA, Miklavcic M (2013) Optimal overlap length in staggered architecture composites under dynamic loading conditions. *J Mech Phys Solids* 61:145–160.

7. Dutta A, Tekalur SA (2014) Crack tortuousity in the nacreous layer–Topological dependence and biomimetic design guideline. *Int J Solids Struct* 51:325–335.
8. Kamat S, Su X, Ballarini R, Heuer A (2000) Structural basis for the fracture toughness of the shell of the conch Strombus gigas. *Nature* 405:1036–1040.
9. Luo W, Bažant ZP (2017) Fishnet statistics for probabilistic strength and scaling of nacreous imbricated lamellar materials. *J Mech Phys Solids* 109:264–287.
10. Bažant ZP, Pang SD (2006) Mechanics-based statistics of failure risk of quasibrittle structures and size effect on safety factors. *Proc Natl Acad Sci USA* 103:9434–9439.
11. Bažant ZP, Pang SD (2007) Activation energy based extreme value statistics and size effect in brittle and quasibrittle fracture. *J Mech Phys Solids* 55:91–131.
12. Bažant ZP, Le JL (2009) Nano-mechanics based modeling of lifetime distribution of quasibrittle structures. *Eng Fail Anal* 16:2521–2529.
13. Bažant ZP, Le JL, Bazant MZ (2009) Scaling of strength and lifetime probability distributions of quasibrittle structures based on atomistic fracture mechanics. *Proc Natl Acad Sci USA* 106:11484–11489.
14. Bažant ZP, Le JL (2017) *Probabilistic Mechanics of Quasibrittle Structures: Strength, Lifetime, and Size Effect* (Cambridge Univ Press, Cambridge, UK).
15. Fisher RA, Tippett LHC (1928) Limiting forms of the frequency distribution of the largest or smallest member of a sample. *Math Proc Cambridge Philos Soc* 24:180–190.
16. Bažant ZP (2005) *Scaling of Structural Strength* (Elsevier Butterworth Heinemann, Oxford).